Error in Prediction due to Data Type Availability in a Coupled Hydro- Mechanical Model

Article

2 authors, including:

J. G. De Aguinaga
Guy Carpenter & Company
2 PUBLICATIONS **7** CITATIONS

SEE PROFILE

Error in Prediction due to Data Type Availability in a Coupled Hydro-Mechanical Model

José Guillermo De Aguinaga
Postdoctoral Research Associate
Research Training Group 1462, Bauhaus-Universität Weimar
Berkaer Str. 9, 99423 Weimar, Germany
e-mail: agui001-ejge@yahoo.com

ABSTRACT

Different types of data provide different type of information. The present research analyzes the error on prediction obtained under different data type availability for calibration. The contribution of different measurement types to model calibration and prognosis are evaluated.
A coupled 2D hydro-mechanical model of a water retaining dam is taken as an example. Here, the mean effective stress in the porous skeleton is reduced due to an increase in pore water pressure under drawdown conditions. Relevant model parameters are identified by scaled sensitivities. Then, Particle Swarm Optimization is applied to determine the optimal parameter values and finally, the error in prognosis is determined. We compare the predictions of the optimized models with results from a forward run of the reference model to obtain the actual prediction errors. The analyses presented here were performed calibrating the hydro-mechanical model to 31 data sets of 100 observations of varying data types. The prognosis results improve when using diversified information for calibration. However, when using several types of information, the number of observations has to be increased to be able to cover a representative part of the model domain. For an analysis with constant number of observations, a compromise between data type availability and domain coverage proves to be the best solution. Which type of calibration information contributes to the best prognoses could not be determined in advance. The error in model prognosis does not depend on the error in calibration, but on the parameter error, which unfortunately cannot be determined in inverse problems since we do not know its real value. The best prognoses were obtained independent of calibration fit. However, excellent calibration fits led to an increase in prognosis error variation. In the case of excellent fits; parameters' values came near the limits of reasonable physical values more often. To improve the prognoses reliability, the expected value of the parameters should be considered as prior information on the optimization algorithm.

KEYWORDS: Embankment, sensitivity analysis, parameter identification, Particle Swarm Optimization.

INTRODUCTION

There has been a growing need to better understand model quality of numerical models in all

branches of science. This issue has been recently addressed by Nishat *et al*. (2012), Keitel and Dimmig-Osburg (2010), Most (2009), Lucas *et al*. (2008) and Babuška *et al*. (2007) among others. Models have grown in complexity and scope. In civil engineering, different models have to be coupled to simulate behavior of complex structures. However, type, location and quality of measurements significantly impact model calibration and their forecast in these coupled models. This information either contributes to model quality by improving model forecast or to model uncertainty when neglecting important information. The models have to be parameterized; however, the values of the parameters are usually not known and have to be calibrated by inverse methods using observations. This study focuses on the influence on model prediction of different observation types for calibration.

To analyze the effects of using different observation types for calibrating a numerical model, a virtual embankment submitted to drawdown conditions will be taken as an example. This is a typical flow and deformation coupled problem in geotechnical engineering. Rapid drawdown conditions can endanger the stability of a water retaining dam. Therefore, observations are usually made under stable, slow drawdown conditions; however, the interest lies in the forecast of the embankment behavior under rapid drawdown conditions.

It is not the goal of this paper to find the best model description for hydro-mechanical models, but to analyze the error related to model calibration under different data type availability conditions. The objective is to identify the data relationships that are necessary to correctly predict deformation, strain and excess pore pressure development within a coupled hydro-mechanical model.

METHODOLOGY

A reference model of a water retaining dam is generated to assess the impact of data availability on model error prognosis. Such a model provides different types of synthetic measurements, in this case, taken under slow drawdown conditions. The same model can be then calibrated to all possible combinations of these measurement sets. Finally, the models with the optimized sets of parameters can be simulated under the scenario of interest, rapid drawdown conditions, and the prognosis error can be compared.

With the reference model we create a total of five different data sets: horizontal and vertical deformation, horizontal and vertical strain and excess pore pressure. Based on these sets we generate 31 combinations ($2^{5\ \text{data types}} - 1 = 31$ data sets) of equal number of observations, but different type of data. In order to determine the effect of "data type" on model forecast, we calibrate the more important parameters to the 31 different data sets using the same model that generated the data. This is necessary to avoid external influences other than data type, and compare their forecast to the reference model.

Before calibration, a sensitivity analysis is performed to determine the most important parameters of the model. The optimal values of the most influential parameters are then identified with Particle Swarm Optimization on a surrogate model. In this optimization, the influential parameters are calibrated to synthetic data using the cumulative average error as the objective function, which norms every time series to account for the different units they might have. By minimizing the average error sum, selected parameters can be calibrated to different types of data. Finally, a simulation using the calibrated models is performed under a rapid drawdown scenario and the actual forecast errors are determined.

Sensitivity Analysis

Local sensitivities are not absolute values; they depend on the initial parameter values and the magnitude of parameter perturbation (Zheng and Bennett, 2002). In this case, the optimum set of

parameters is known from the reference model. Since there is no uncertainty on the value of the parameters, local scaled sensitivities ($ss^{+}_{i,j}$) are used to determine the most relevant parameters of the model. Otherwise, global sensitivity methods (Saltelli *et al.*, 2008) should be applied to provide reliable estimators over different order of magnitude in parameter space. Local sensitivities provide the ratio of difference in model response at each i measuring point (y_i) to a small change in parameter value of every j parameter (p_j) where $i, j \in \mathbb{N}$. They are calculated as in Zimmerer (2010) as follows:

$$ss^{+}_{i,j} = \frac{\partial y_i}{\partial p_j}\frac{p_j}{y_i} \tag{1}$$

In matrix form, the scaled sensitivity matrix ($\mathbf{SS}^{+}$) can be calculated as

$$\mathbf{SS}^{+} = \frac{\partial \mathbf{y}}{\partial \mathbf{p}}\frac{\mathbf{p}}{\mathbf{y}} \tag{2}$$

where $\mathbf{y}$ is the calculated model response vector $\{y_1, y_2, ..., y_i\}$ and $\mathbf{p}$ is the model parameter vector $\{p_1, p_2, ..., p_j\}$.

The partial derivatives are approximated by forward finite difference:

$$\frac{\partial \mathbf{y}}{\partial \mathbf{p}} \approx \frac{\mathbf{y}(\mathbf{p}+\Delta\mathbf{p})-\mathbf{y}(\mathbf{p})}{\Delta\mathbf{p}} \tag{3}$$

The resulting sensitivities are ranked calculating the variance-covariance matrix, $(\mathbf{SS}^{+T}\mathbf{SS}^{+})^{-1}$, which is the inverted product of the transposed scaled sensitivity matrix multiplied by itself. The smaller the value of the respective parameter in the main diagonal of the variance covariance matrix, the more influential the parameter is.

Optimization

The divergence between model response and reference values (observations) is quantified by the objective function as follows:

$$F(\mathrm{p}) = \sqrt{\sum_{i=1}^{n} \frac{(y_{i,meas}-y_i(p_1,p_2,...,p_n)_{calc})^2}{\sum_{i=1}^{n} y_{i,meas}^2} w_i} \tag{4}$$

where $F(\mathrm{p})$ is the average error sum, $i = 1, 2, ..., n$ counts each measurement of a time series, and w is a weighting factor, in this case equal to one. The units of the values in the objective function are being canceled by norming the squared residuals at each measuring point (numerator Equation 4), by the squared sum of the measurements at the given point (denominator).

An automated calibration is performed with Particle Swarm Optimization (Kennedy and Eberhard, 1995) on a surrogate model. Here, the numerical model is approximated by a fully quadratic function (Zimmerer *et al.*, 2011):

$$y(\mathrm{p})_{calc} = \hat{y}(\mathrm{p}, \beta) + \hat{\epsilon} \tag{5}$$

where β are the coefficients of the fully quadratic approximation and $\hat{\epsilon}$ is the error between numerical and surrogate model.

During optimization the sum of the objective function for each measurement series is minimized:

$$F_{total}(\mathrm{p}) = \frac{1}{m}\sum_{j=1}^{m} F_j(\mathrm{p}) \rightarrow min. \tag{6}$$

where *m* stands for the amount of measurement series.

ILLUSTRATIVE EXAMPLE: WATER RETAINING DAM

A numerical model of a water retaining dam under drawdown conditions is used to illustrate the influence of data availability on error prognosis. The example is based on the PLAXIS 2D Tutorial *stability of dam under rapid drawdown* (PLAXIS, 2010a) which is slightly modified for this study. The simulations were performed with PLAXIS 2D (Brinkgreve *et al*., 1997-2010), a commercial Finite Element Program.

Geometry and Boundary Conditions

The earth dam is of trapezoidal form (Figure 1), with a height of 30 m, an upper side of only 5 m length, and a bottom length of 172.5 m, of which 20 m correspond to the core of the dam. The underlying block is 260 m in length and also 30 m in height. The dimensions of the block were conceived in order to avoid boundary conditions from affecting the results inside the dam.

A mesh was constructed with 6-node triangular elements refined on the embankment itself. On Figure 1, the initial water level at 25 m is marked by the solid line and the final water level at 5 m is represented by the dashed line.

Furthermore, the boundary condition at the bottom of the rectangular block is of full fixity, no deformation in horizontal or vertical direction allowed. At the sides just vertical deformation is allowed, while the entire upper boundary is a free surface with a time dependent water level.

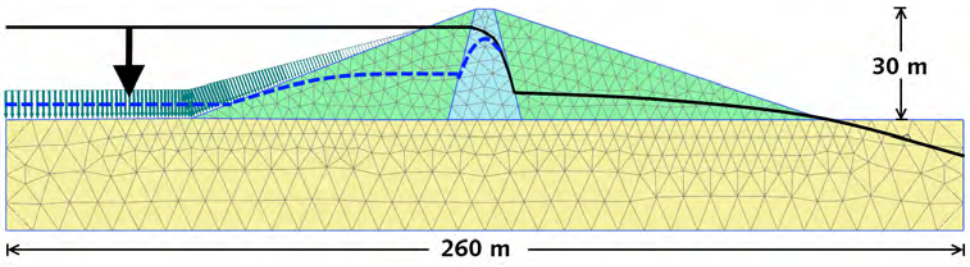

Figure 1: Mesh of water retaining dam with core (trapezoid in the center), fill (lateral triangles) and subsoil (rectangular basement), showing schematic drawdown and water pressure distribution.

Material Model

The embankment has three distinctive materials which have to be parameterized: 1) an almost impermeable clay core to prevent flow through it; 2) the fill, usually constructed of local material to protect the core from erosion and forces applied by the water; and 3) the subsoil which is the foundation on which the dam is built on.

For all three soil materials, the Mohr-Coulomb model (MC) is used to represent the elastic-plastic soil behavior. MC is suitable to analyze the stability of slopes and embankments (Ti *et al*., 2010). The

hydraulic model is parameterized using the Hypres data set available in PLAXIS with Van Genuchten parameterization. This parameterization is of coarse subsoil type for fill and subsoil material and of very fine type for the core. When using the MC model to simulate material behavior, the hydro-mechanical coupling is not perfect. It does not account for an increase in stiffness in the unsaturated zone due to the effects of dewatering. This property is only considered by the Barcelona Basic Model under consolidation calculation, as demonstrated in Galavi (2010).

Nevertheless, this hydro-mechanical model is taken as a reference model and therefore, assumed to be the truth. This is indeed correct, since it generates the synthetic data used in the present study. However, if the engineer faces a real structure, has real data and is not sure which model would be adequate, there are model selection methods such as AIC or Bayesian Model Selection to identify the most suitable model, see De Aguinaga (2010) and Keitel (2012).

The values of the model parameters are given in Table 1 and are synthetic, since they were not determined from an existing structure.

Table 1: Soil parameter values for the three different materials.

Soil parameters		Core	Fill	Subsoil
		Undrained A	Drained	Drained
Saturated soil unit weight	γ [kN/m^3]	16	16	17
Unsaturated soil unit weight	γ [kN/m^3]	18	20	21
Shear modulus	G [kN/m^2]	555.60	7518.80	19230.77
Poisson's ratio	ν' [-]	0.35	0.33	0.30
Cohesion	C' [kN/m^2]	5	5	1
Friction angle	φ' [°]	25	31	35
Dilatancy angle	ψ [°]	0	1	5
Hydraulic conductivity (isotropic)	k_{xy} [m/d]	0.0001	0.25	0.01

In the PLAXIS Undrained A condition, stiffness and strength are defined in terms of effective properties; the soil as a whole is made incompressible by automatically applying a large bulk stiffness to the water, and excess pore pressure is also calculated in the unsaturated zone (PLAXIS, 2010b).

Simulation

The hydraulics in PLAXIS are simulated according to the Darcy law for fully saturated soil and with the Richards equation, which describes unsaturated groundwater flow. They are coupled to the mechanical model using Biot's theory of consolidation, neglecting an increase in stiffness of the dewatered zone. Biot's formulation contains a coupled hydro-mechanical behavior represented by both the equilibrium equation and the continuity equation of the water-soil mixture (Galavi, 2010).

Calculations are performed in the classical mode, which uses Terzaghi's definition of stress. In the first phase, the initial stress due to the soil and material weight is calculated, as well as the initial pore water pressure under undrained behavior and steady state groundwater flow conditions. Following the previous Gravity loading phase is a Nil-Step phase. This PLAXIS simulation phase improves the accuracy of the equilibrium stress field with a plastic drained long term calculation in which no additional loading is applied (PLAXIS, 2010c). Finally, the effect of the drawdown can be simulated as a consolidation phase with transient groundwater flow, in which the dam is submitted to a linear drawdown of 40 cm/d.

RESULTS AND CONCLUSION

Sensitivities

Eight nodes and five stress points within the core and the fill (Figure 2) were selected for measurements of five different types of data: horizontal and vertical deformation (u_x, u_y), horizontal and vertical strain (ε_{xx}, ε_{yy}) and excess pore pressure (*EPP*). Deformation and strain are correlated and therefore, information gain is maximized by measuring them at different locations.

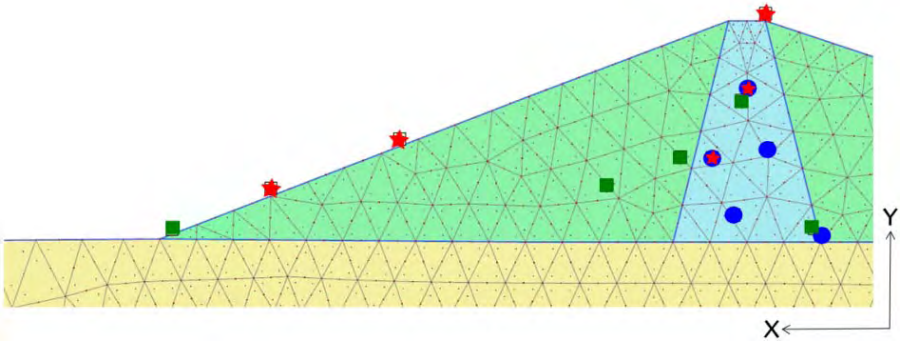

Figure 2: Observation points at the embankment for sensitivity analysis (u_x, u_y: red star; ε_{xx}, ε_{yy}: green square and *EPP*: blue circle).

The sensitivities were calculated for all soil parameters of the three materials with respect to the five different types of model answers at the observation points shown in Figure 2. The resulting parameters of interest for the present study were those of the soft soil core, especially the isotropic hydraulic conductivity (k_{xy}), two parameters from Hooke's law: shear modulus (G) and Poisson's ratio (ν') and also the parameter that describes the flow rule, the dilatancy angle (ψ). Since we are working in the range of values where the dam is stable and cannot sample data from its collapse, the parameters that define failure were not of interest for this study. These are the friction angle and cohesion. The resulting variance-covariance matrix of the most influential parameters is shown in Table 2. The smaller the value of the diagonal, the more sensitive the respective parameter is. The most influential parameter is k_{xy} from the hydraulic model followed by ν' and G from Hooke's law of the material model.

Table 2: Variance-Covariance Matrix $(\mathbf{SS}^{+T}\mathbf{SS}^{+})^{-1}$ of the most influential parameters of the impermeable core.

	G	v'	ψ	$\lg(k_{xy})$
G	$\mathbf{2{\cdot}10^{-3}}$	$-8{\cdot}10^{-4}$	$1{\cdot}10^{-2}$	$-1{\cdot}10^{-5}$
v'		$\mathbf{4{\cdot}10^{-4}}$	$-6{\cdot}10^{-3}$	$6{\cdot}10^{-6}$
ψ			$\mathbf{9{\cdot}10^{-2}}$	$-9{\cdot}10^{-5}$
$\lg(k_{xy})$		symmetric		$\mathbf{3{\cdot}10^{-7}}$

Calibration

The four previous parameters, which were the most influential to a set of model answers of diverse types in 13 different points, were calibrated to different data type availability. 31 data sets, shown in Table 3, each with 100 observations were generated from the combinations of u_x, u_y, ε_{xx}, ε_{yy} and *EPP*.

Table 3: Possible combinations of data type availability for calibration purpose using 100 observations; number of points per data type (10 measurements in time per point) and resulting average error sum [%].

	1	2	3	4	5	6	7	8	9	10	11	12	13	14	15	16
u_x	2	3	2	2	3		3	3	3	4	3	3				
u_y	2	2	2	2		3	3	3	3				4	3	3	
ε_{xx}	2	3	3		2	2	4			3	3		3	3		3
ε_{yy}	2	2		3	2	2		4		3		3	3		3	3
EPP	2		3	3	3	3			4		4	4		4	4	4
Error	0.8	0.2	0.6	0.9	0.9	1.0	0.1	0.1	0.9	0.3	0.9	0.3	0.0	1.1	0.7	1.4

	17	18	19	20	21	22	23	24	25	26	27	28	29	30	31	
u_x	5	5	5	5							10					
u_y	5				5	5	5					10				
ε_{xx}		5			5			5	5				10			
ε_{yy}			5			5		5		5				10		
EPP				5			5		5	5					10	
Error	0.2	0.0	0.2	0.1	0.1	0.6	0.7	0.2	1.1	1.7	0.1	0.2	0.9	0.7	1.5	

An attempt was made to equally distribute the number of points selected for each data type while maintaining 100 observations and time series of 10 measurements. This works well for 1, 2 and 5 data types (see combination 1 and 17 to 31 in Table 3). However, when using 3 or 4 data types (combinations 2 to 16) selecting the same number of nodes will result in a value of observations different than 100. Therefore, the number of nodes was increased by one in the data type which was considered to be under represented, e.g. ε_{xx} in combination 7.

The resulting combinations have a constant number of observations and vary in data type. This generates a trade-off between data type coverage and spatial domain coverage. The spatial coverage of the first data set, considering all data types (first data set of Table 3) is shown at the left side of Figure 3. Measured in two nodes are u_x and u_y (shown as red stars), *EPP* also in two nodes (shown as blue circles), and ε_{xx} and ε_{yy} in two stress points (shown as green squares). In contrast, at the right side of Figure 3, data set 31, which uses just *EPP* observations, shows a good spatial coverage of *EPP* in the core. As data type increases, spatial coverage decreases and vice versa.

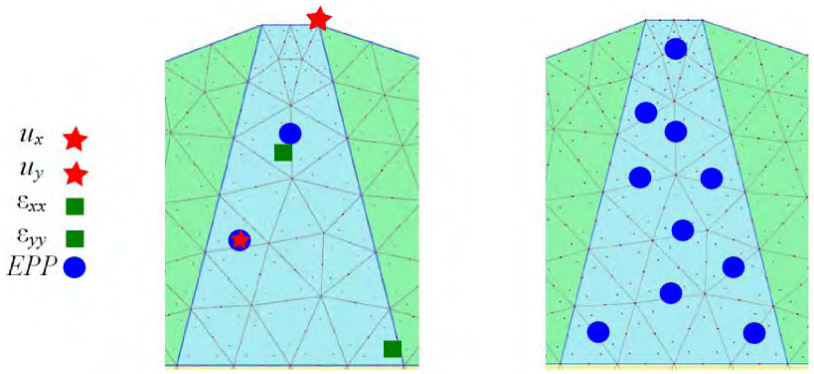

Figure 3: Left: Observation points for data set 1;
Right: Observation points for data set 31 of Table 3.

The model was calibrated to the 31 data sets with an automated algorithm using the Particle Swarm Optimization method on a surrogate model. The resulting deviations to the respective data sets are also given in Table 3 as average error sum in percent.

The average error sum for all different calibrations is small, lower than 2 %. Calibration results are sorted in descending average error and in groups of number of data types used for calibration (Figure 4). Notice that due to sorting, the x-axis of the figure does not correspond any more with the combination sets of Table 3. Some optimizations had excellent fit, up to 0.3 % average error (green frame), a second group with good fit on the range 0.5 - 1.2 % average error (orange frame), and a third group with relative poor fit from 1.4 to 1.7 % average error (red frame). Most of the calibrations fall within the first two classes. A reason for the low calibration errors is that no noise is considered in the data.

Furthermore, from Figure 4, we can determine that the best results are obtained by using 1 to 3 data types, however, also the worst values. The choice of data type makes then the difference between best or worst case. It must be noticed that most of the best calibration results can be obtained with 2 and 3 data types. This reflects the trade-off between using different data types for calibration vs. the spatial coverage of each single data type. For our case, in which the number of observations is fix, a set with two or three data types, might allow for variety in information for calibration while maintaining some representative spatial coverage of the domain.

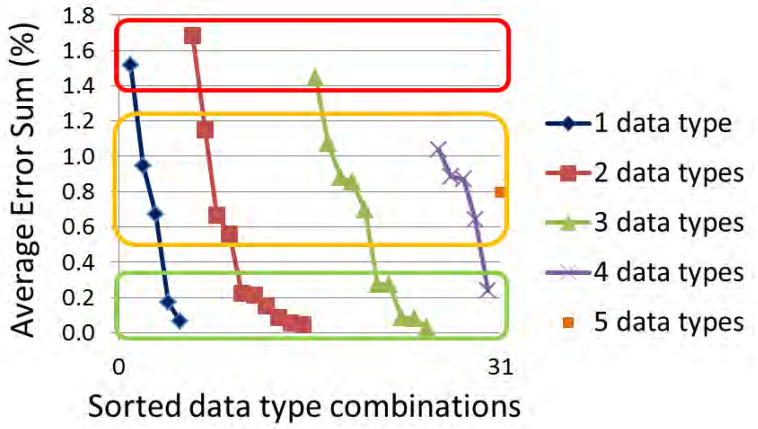

Figure 4: Sorted average error sum of calibration results by number of data type used.

In Figure 5, the same results are sorted by each of the five data types used for calibration. Every data type is used 16 times in different combinations. The calibrations using combinations of data sets with u_x show most of the time a better fit than without. In contrast, the fit is usually worst when *EPP* is considered for calibration.

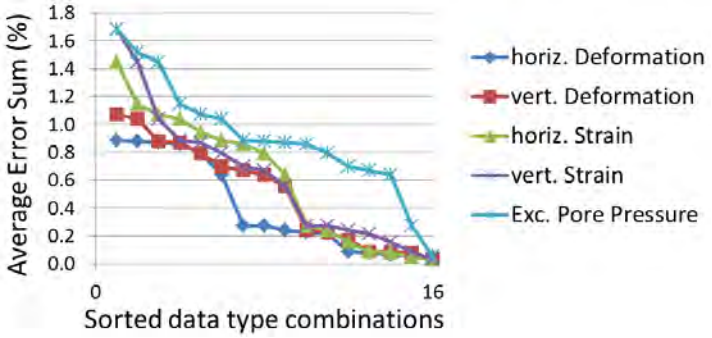

Figure 5: Sorted average error sum of calibration results by data type.

Forecast Simulations

A prognosis of the model was carried out for each of the resulting optimal parameter values. For this, 90 observations were taken over a 5 day period in which the water table decreased at a linear rate of 4 m per day.

The average error sums of the forecast were lower than those obtained during calibration. However, the average error sums of both graphs are not comparable in magnitude, since the prognosed values were measured at different points, at different times, with fewer measurements and, more importantly with other boundary conditions (rapidly falling water table). However, tendencies can be compared to discover any correlations.

The forecast results are displayed in Figure 6. The average error sum of the prognosis is sorted also by number of data types, and we see a similar trend as with the calibration results. The best and worst fit are obtained with 2 or 3 types of data. The maximum prediction average error sum was around 1 %. Most of the forecast results fall within the range 0.3 and 0.7 % average error sum.

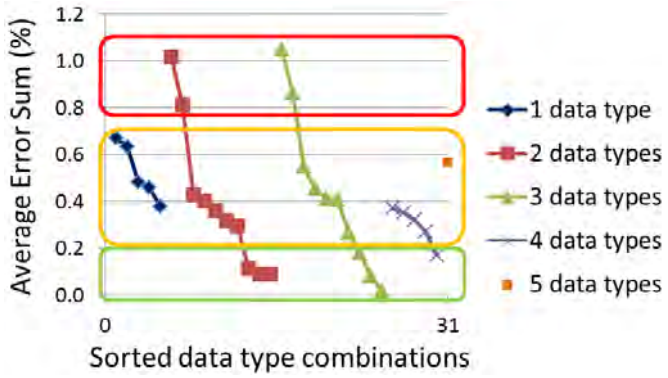

Figure 6: Sorted average error sum of forecast results by number of data type used.

The parameters responsible for the best and worst cases are appreciable in Figure 7, where the results are sorted by type of observation used for calibration. Surprisingly, the worst prognoses were made by considering deformation or strain observations during calibration. In contrast, a guarantee for good prognosis seemed to be attained by calibration with *EPP* information. This opposes the deductions from Figure 5, in which calibrating with deformation while excluding *EPP* information is recommended to obtain best calibration results.

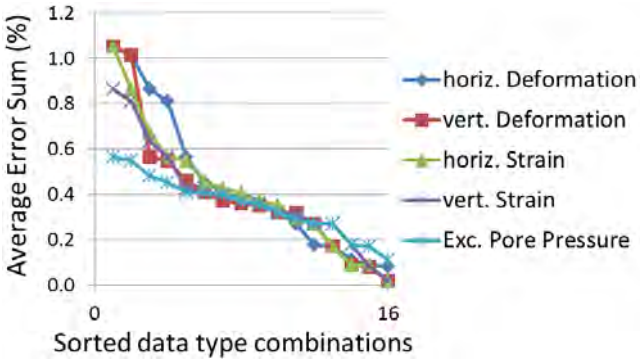

Figure 7: Sorted average error sum of forecast results by data type.

By plotting now the sorted calibration results against their actual errors of the prognosis (left side of Figure 8), we observe that a decrease in calibration error does not improve the prognosis accuracy. The prognosis error seems to be normally distributed around 0.4 % average error sum. However, for the case of excellent calibration fit with average error sums lower than 0.3 %, the validation error becomes more variable, and the parameter set is susceptible to give a prognosis with higher errors.

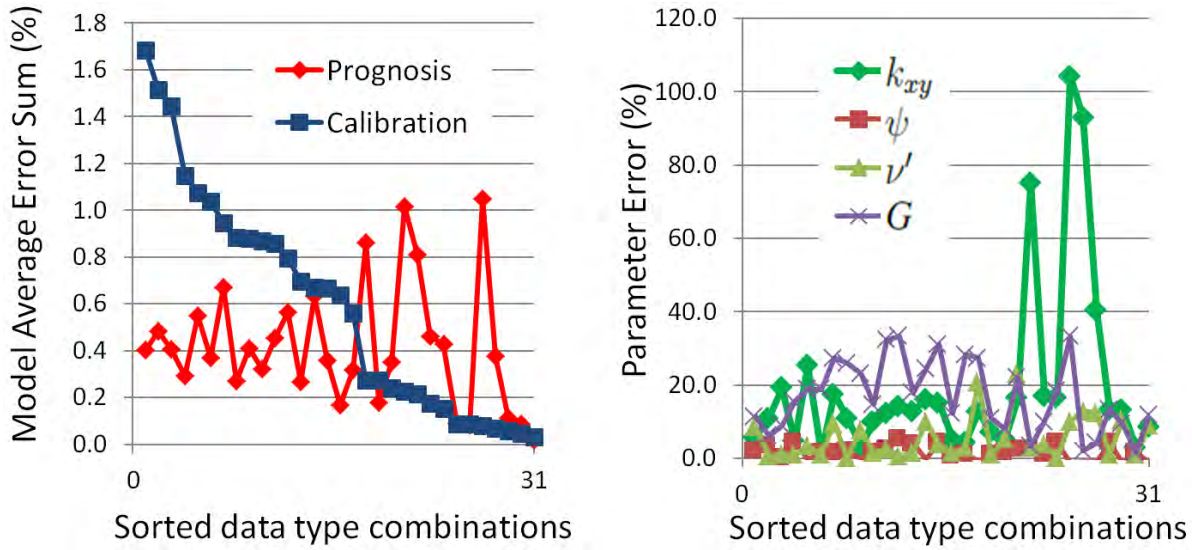

Figure 8: Left: sorted average error sum of calibration results with corresponding prognosis error. Right: Corresponding parameter errors.

The right side of Figure 8 shows the corresponding parameter error of the optimized parameter sets at the left side of the figure. By very small calibration errors, the optimized parameter values can be driven to values close to the limit of reasonable physical values, as it was here the case for several combinations for k_{xy}, which is the most sensitive parameter in this model.

CONCLUSION

The fit obtained by the automated Particle Swarm Optimization calibration was very good, with an average error sum in all cases lower than 2 %. However, the error in prognosis does not correlate with the calibration effort, since when calibration error decreases, validation error does not. Interestingly, excellent calibration values led to an increase in prognosis error variation. These calibrations, with very small errors, can drive the value of the optimized parameters to the limit of reasonable physical values, as it is here the case. The error of the prognosis depends on the parameter error and since we do not know the real value of the parameter in an inverse problem, the parameter error cannot be determined.

Surprisingly, the model calibrated to all five different types did not provide the best results. This could be explained by the reduction of the spatial coverage. Best and worst calibration results were obtained using 2 or 3 types of information. Depending on which data sets are considered, either the best or the worst results are obtained. The best calibrations usually were obtained considering u_x, while the worst calibrations included a data set of *EPP*. The opposite was the case for the prognosis. Good prognoses were attained with the data sets which considered *EPP* for calibration, while the worst prognoses were given by those considering u_x for calibration. The information that contributes to the best prognoses could not be determined in advance. Both, information diversity for calibration and a good coverage of model domain are important for good prognoses. In order to obtain better prognoses, it is preferable to accept higher calibration errors and obtain optimized parameter values which are more likely to be expected, than excellent calibration fit with unreasonable parameter values. This could be implemented in an automated optimization algorithm by using the expected value of the parameters as prior information for calibration, as in Jakeman *et al*. (2006).

AKNOWLEDGMENTS

The author would like to acknowledge the support of Dr. Martin Zimmerer for allowing the use of his optimization code VARO^{2}PT, which interacts with PLAXIS and the support of the German Research Foundation (DFG) through the Research Training Group 1462.

REFERENCES

1. Babuška, Ivo, F. Nobile and R. Tempone (2007) "Reliability of Computational Science," Numerical Methods for Partial Differential Equations, Vol. 23, No. 4, pp 753-784, doi:10.1002/num.20263.
2. Brinkgreve, Ronald B. J., W. M. Swolfs, E. Engin, D. Waterman, A. Chesaru, P. G. Bonnier and V. Galavi (1997-2010) "PLAXIS 2D 2010 (version 2010.01)," Delft, Netherlands: PLAXIS b.v, available at http://www.plaxis.nl.
3. De Aguinaga, José G. (2010) "Uncertainty Assessment of Hydrogeological Models Based on Information Theory," Dissertation, Technische Universität Dresden, available at http://nbn-resolving.de/urn:nbn:de:bsz:14-qucosa-71814.
4. Galavi, Vahid. (2010) "Groundwater flow, fully coupled flow deformation and undrained analyses in PLAXIS 2D and 3D," Tech. rep., Delft, Netherlands: PLAXIS b.v. Research Department, available at http://kb.plaxis.nl/author/v-galavi.
5. Jakeman, Anthony J., R. A. Letcher and J. P. Norton (2006) "Ten iterative steps in development and evaluation of environmental models," Environmental Modelling & Software, Vol. 21, No. 5, pp 602-614, doi:10.1016/j.envsoft.2006.01.004.
6. Keitel, Holger (2012) Evaluation Methods for Prediction Quality of Concrete Creep Models, In: Schriftenreihe des DFG Graduiertenkollegs 1462 Modellqualitäten, Vol. 2, Dissertation, Bauhaus-Universität Weimar, available at http://nbn-resolving.de/urn:nbn:de:gbv:wim2-20120207-15569.
7. Keitel, Holger and A. Dimmig-Osburg (2010) "Uncertainty and sensitivity analysis of creep models for uncorrelated and correlated input parameters," Engineering Structures, Vol. 32, No. 11, pp 3758-3767, doi:10.1016/j.engstruct.2010.08.020.
8. Kennedy, James and R. Eberhard (1995) "Particle Swarm Optimization," in: Proc. IEEE International Conference on Neuronal Networks, Perth, Australia, 27 Nov. - 01 Dec. 1995, pp 1942-1948.
9. Lucas, Leonard J, H. Owhadi and M. Ortiz (2008) "Rigorous verification, validation, uncertainty quantification and certification," Comput. Methods Appl. Mech. Engrg., Vol. 197, pp 4591-4609, doi:10.1016/j.cma.2008.06.008.
10. Most, Thomas (2009) "Estimating uncertainties from inaccurate measurement data using maximum entropy," in: K. Gürlebeck and C. Könke (Eds.), 18th International Conference on the Application of Computer Science and Mathematics in Architecture and Civil Engineering, Weimar, Germany, 07-09 July 2009.
11. Nishat, Shazia ,Y. Guo and B. W. Baetz (2012) "Relative Importance of Input Parameters in the Modeling of Soil Moisture Dynamics of Small Urban Areas," Journal of Hydrologic Engineering, Vol. 17, No. 3, pp 359-367, issn: 1084-0699/2012/3-359-367.

12. PLAXIS b.v. (2010a) "PLAXIS 2D tutorial manual 2010," Tech. rep., Delft, Netherlands, available at http://www.plaxis.nl/shop/135/info/manuals/.
13. PLAXIS b.v. (2010b) "PLAXIS material models manual 2010," Tech. rep., Delft, Netherlands, available at http://www.plaxis.nl/shop/135/info/manuals/.
14. PLAXIS b.v. (2010c) "PLAXIS scientific manual 2010," Tech. rep., Delft, Netherlands, available at http://www.plaxis.nl/shop/135/info/manuals/.
15. Saltelli, Andrea, M. Ratto, T. Andres, F. Campolongo, J. Cariboni, D. Gatelli, M. Saisana and S. Tarantola (2008) "Global Sensitivity Analysis. The Primer," John Wiley & Sons, isbn: 978-0470059975.
16. Ti, Kok S., B. B. K. Huat, J. Noorzaei, M. S. Jaafar and G. S. Sew (2009) "A Review of Basic Soil Constitutive Models for Geotechnical Application," Electronic Journal of Geotechnical Engineering, Vol. 14, Bund. J, pp 1-18.
17. Zheng, Chunmiao and G. D. Bennett (2002) "Applied Contaminant Transport Modeling," 2nd ed., New York, USA: John Wiley & Sons, isbn: 0471384771.
18. Zimmerer, Martin M. (2010) "Identifikation konstitutiver Parameter von weichen feinkörnigen Böden, Beitrag zum Konsolidationsverhalten von Ton," In: Schriftenreihe des DFG Graduiertenkollegs 1462 Modellqualitäten, Vol. 1, Dissertation, Bauhaus-Universität Weimar, Germany.
19. Zimmerer, Martin M., T. Schanz, Y. Lins and V. Bettzieche (2011) "Numerical Analysis of Water Reservoir Dam - Prediction of Long Term Performance of Versetal dam (Germany)," 79th ICOLD Annual Meeting, Lucerne, Switzerland, May 29 - June 3, 2011.